Hybrid model for AC Losses in High Speed PMSM for arbitrary flux density waveforms

Conference Paper · August 2020

DOI: 10.1109/ICEM49940.2020.9271017

6 authors, including:

Taha El Hajji
Ecole normale supérieure de Cachan
4 PUBLICATIONS **21** CITATIONS
SEE PROFILE

Sami Hlioui
CY Cergy Paris Univérsité - SATIE Laboratory
86 PUBLICATIONS **977** CITATIONS
SEE PROFILE

François Louf
Ecole normale supérieure de Cachan
62 PUBLICATIONS **401** CITATIONS
SEE PROFILE

Mohamed Gabsi
Ecole normale supérieure de Cachan
238 PUBLICATIONS **4,271** CITATIONS
SEE PROFILE

Hybrid model for AC Losses in High Speed PMSM for arbitrary flux density waveforms

Taha El Hajji, Sami Hlioui, François Louf, Mohamed Gabsi, Guillaume Mermaz-Rollet and M'Hamed Belhadi

***Abstract* -- Increasing speed of electric machine leads to high losses especially in stator winding assembly due to eddy currents effect. Commonly adopted formula for AC losses calculation tends to be applicable in the case of sinusoidal flux density. In this paper, a hybrid model predicting AC winding losses is presented based on one slot per pole of surface-mounted permanent-magnet machines using two formula taking into account the true flux density waveform. The results obtained comply with finite-elements results. The hybrid model was also used to investigate the influence of tooth-tip on AC losses.**

***Index Terms*-- AC losses, high speed, electric machines, proximity effect, skin effect**

I. NOMENCLATURE

R_{DC}	DC resistance of conductor
l	Length of conductor
S	Surface of conductor
d	Conductor diameter
R_{skin}	Resistance due to skin effect
I_{RMS}	RMS value of current
δ	Skin depth
μ_0	Permeability of free space
σ	Conductivity of copper
ber	Real part of first kind Bessel function
bei	Imaginary part of first kind Bessel function
f	Frequency of signal
T	Period of signal
ω	Pulsation of signal
ω_i	Pulsation of i^{th} harmonic
B_{global}	Global flux density
B_{ext}	External flux density
$B_{ext,m}$	Maximum value of B_{ext}
$B_{i,m}$	Maximum value of B_i
B_r	Radial component of flux density
B_θ	Tangential component of flux density
$B_{r_{i,m}}$	i^{th} Harmonic of B_r
$B_{\theta_{i,m}}$	i^{th} Harmonic of B_θ
d_{lim}	Conductor's diameter limit to verify assumption
J	Current density in conductor
J_s	Current density in conductor due to skin effect
J_p	Current density in conductor due to proximity effect
P_i	Proximity losses due i^{th} harmonic of flux density

II. INTRODUCTION

THE need of lightweight electric machines especially for electric vehicle applications led to increase researches on high speed [1], [2], [3]. In order to have an accurate model of the electrical machine and especially for the prediction of power loss, a special attention should be given to AC losses in windings as they become significant at high frequency [4]. This is due to eddy currents induced by the magnetic field created by the current-carrying conductor known as skin effect and the external magnetic field known as proximity effect [5]. Previous works allow predicting AC losses in transformer windings [6], [7]. However, AC losses prediction in electric machines is more complicated due to the presence of rotating flux density generated by the rotation of magnets [5], which occurs even at no load and increases at high frequency [8] and at large slot openings.

In order to calculate AC winding losses, many methods exist in literature. Finite element method (FEM) allows a high accuracy of results but are time consuming [9], [10]. In order to reduce the computation time, different models have been developed. Reference [8] studied AC losses in windings with rectangular and round conductors and for different layouts in a permanent magnet synchronous machine (PMSM). Reference [9] studied the influence of winding layer number on AC losses in a surface-mounted PMSM. On the other side, analytical methods are fast but are used for special geometries and based on certain hypothesis [11], [12], [13], [14], [15]. Reference [11] developped a 1-D analytical model to predict AC losses in a PMSM. Reference [16] developed a 1-D and 2-D analytical models for AC losses in the case of rectangular slots. Reference [17] presented an analytical method based on Poynting vector for any slots form. Unfortunately, all these methods, excepting FEA, cannot take into account the alternating flux density due to rotation of magnets and are applicable only for sinusoidal flux density. By combining FEM and analytical methods, known as hybrid methods, it is possible to overcome the weaknesses of both methods and give accurate results with less computation time. Reference [18] presented a hybrid model to study AC losses in windings at high frequency however this model is based on the assumption that flux density is sinusoidal. A care must also be given to the fact that the magnetic field density distribution inside the slots are two-dimensional [7].

The objective of this paper is to present a hybrid method considering arbitrary waveform of flux density and its two components in order to calculate accurately AC winding losses using two formulae. Section III presents formula of skin effect for sinusoidal current supply, two formulae of proximity effect for arbitrary waveforms of flux density

This work was supported in part by the OpenLab "Electrical Engineering For Mobility", Groupe PSA, France

Taha El Hajji is with SATIE, CNRS, Groupe PSA, ENS Paris-Saclay, Gif-sur-Yvette, France (taha.elhajji@mpsa.com)

Sami Hlioui is with SATIE, CNRS, CNAM, ENS Paris-Saclay, Gif-sur-Yvette, France (sami.hlioui@satie.ens-cachan.fr)

François Louf is with LMT, CNRS, ENS Paris-Saclay, Gif-sur-Yvette, France (francois.louf@ens-paris-saclay.fr)

Mohamed Gabsi is with SATIE, CNRS, ENS Paris-Saclay, Gif-sur-Yvette, France (mohamed.gabsi@ens-cachan.fr)

Guillaume Mermaz-Rollet is with Groupe PSA, 78140 Vélizy, France (guillaume.mermazrollet@mpsa.com)

M'Hamed Belhadi is with Groupe PSA, 78955 Carrières-Sous-Poissy, France (mhamed.belhadi@mpsa.com)

considering its two components, and the orthogonality principle. Then, in section IV AC losses calculations are conducted on one slot per pole surface mounted PMSM at both no load and on load conditions for different values of conductor's diameter and frequency. Obtained results are compared with 2-D FEM ones. Finally, the influence of slot opening on the accuracy of AC losses prediction by this hybrid model is investigated.

III. Technical Work Preparation

Windings losses are composed of 3 terms: proximity effect, skin effect and circulating currents. In our study, we will use one strand in hand, hence, the latter effect will not be considered. In order to evaluate the related losses, formulae of both skin and proximity effect losses are presented as well as their hypothesis. The two components and the arbitrary waveform of flux density are taken into account. The orthogonality principle is then presented which allows summing both skin and proximity losses.

A. Skin Effect Model

Skin effect is due to eddy currents induced by the magnetic field H_{AC} created by the sinusoidal current-carrying conductor as shown in Figure 1. The current is then concentrated near the surface as shown by the grey surface in Figure 1, which increases the equivalent electrical resistance.

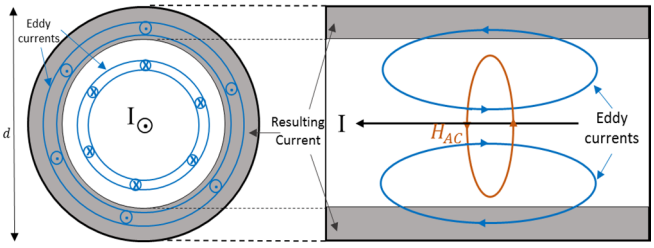

Figure 1 Eddy currents induced in round conductor and resulting current due to skin effect

Resistance in case of DC current is expressed as follows:

$$R_{DC} = \frac{l}{\sigma S} \tag{1}$$

We assume that eddy currents are resistance limited and the end effects are neglected. Hence, the ratio between the real resistance value (AC resistance) due to skin effect and DC resistance can be expressed as follows [19]:

$$\frac{R_{skin}}{R_{DC}} = \frac{\gamma}{2} \cdot \frac{ber(\gamma)bei'(\gamma) - bei(\gamma)ber'(\gamma)}{ber'^2(\gamma) + bei'^2(\gamma)} \tag{2}$$

Joule Losses in the case of DC current are expressed as follows:

$$P_{DC} = R_{DC} . I_{RMS}^2 \tag{3}$$

Losses due to skin effect for sinusoidal current supply can be expressed as follows [19]:

$$P_{skin} = R_{skin} . I_{RMS}^2 \tag{4}$$

Where,

$$\gamma = \frac{d}{\delta\sqrt{2}} \tag{5}$$

$$\delta = \frac{1}{\sqrt{\pi f \mu_0 \sigma}} \tag{6}$$

The ratio between AC resistance and DC resistance in function of γ is shown in Figure 2. Skin effect is noticeable for values of γ above 1.5 which is equivalent to:

$$d > 1{,}5.\sqrt{2}.\delta \approx 2{,}12 \times \delta \tag{7}$$

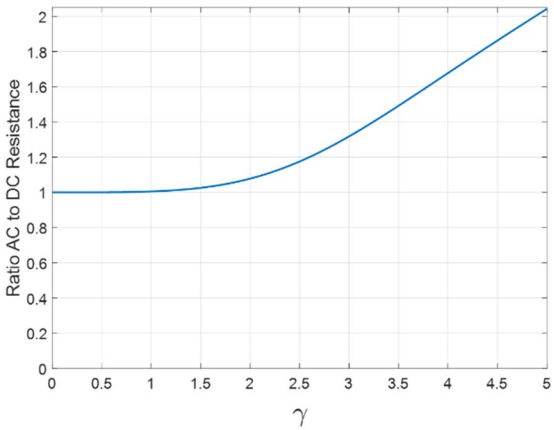

Figure 2 Ratio of AC resistance to DC resistance in function of γ

Above formula of skin effect losses is only applied for sinusoidal current. However, in order to take into account arbitrary current waveform, losses due to each harmonic are summed [20].

B. Proximity Effect Model

Proximity effect is due to eddy currents induced by an external magnetic field B_{ext} created by neighbouring conductors and/or magnets rotation/movement. Due to induced eddy currents, shown in Figure 3, the current flowing in the conductor will be concentrated on one side. Hence, the resistance increases.

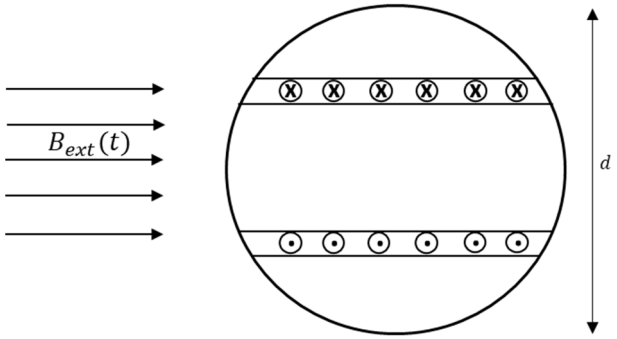

Figure 3 Induced Eddy Currents in round conductor due to external alternating magnetic field

In the presented model, we are going to assume that:

- Flux density B is uniform on conductor,
- Eddy currents are resistance limited,
- External magnetic field B_{ext} is assumed to be equal to global magnetic field B_{global}, that includes contribution of the conductor, evaluated by FEM.

The value of flux density, considered uniform, is taken in the center of conductor.

Many previous works use the following formula of power proximity losses under the assumption of sinusoidal flux density:

$$P_{proximity} = \frac{\pi\sigma l d^4 B_{ext,m}^2 \omega^2}{128} \tag{8}$$

Reference [7] presents the instantaneous power proximity losses for arbitrary waveform of flux density:

$$p_{proximity}(t) = \frac{\pi\sigma l d^4}{64}\left(\frac{dB_{ext}}{dt}\right)^2 \tag{9}$$

According to Parseval's identity, we can use the following formula that allows evaluating the contribution of each harmonic of flux density:

$$P = \sum_i P_i = \sum_i \frac{\pi\sigma l d^4 B_{i,m}^2 {\omega_i}^2}{128} \quad (10)$$

Where i means the index of i^{th} harmonic of flux density Fourier series.

While flux density is two-dimensional in electric machine's slots, formulae (9) and (10) will be applied to both radial B_r and tangential B_θ components of flux density [21]:

$$P_{proximity} = \frac{1}{T}\int \left(\frac{\pi\sigma l d^4}{64}\left(\frac{dB_r}{dt}\right)^2 + \frac{\pi\sigma l d^4}{64}\left(\frac{dB_\theta}{dt}\right)^2\right) dt \quad (11)$$

$$P_{proximity} = \sum_{i^{th}\ harmonic} \left(\frac{\pi\sigma l d^4 {B_r}_{i,m}^2 \omega_i^2}{128} + \frac{\pi\sigma l d^4 {B_\theta}_{i,m}^2 \omega_i^2}{128}\right) \quad (12)$$

The assumption of uniform flux density B on conductor is equivalent to:

$$d \ll \delta \quad (13)$$

In order to verify (13), a range of conductor's diameter is considered in this study and will be validated later in this paper:

$$d < d_{lim} = 0{,}5 \times \delta \quad (14)$$

Figure 4 shows the limit of conductor's diameter in function of frequency in order to verify (14).

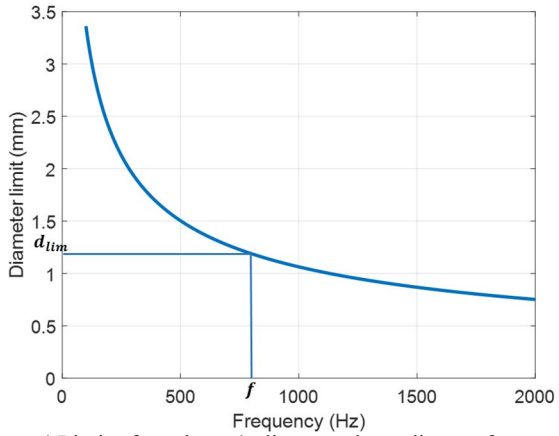

Figure 4 Limit of conductor's diameter depending on frequency in order to verify assumption of B uniform on conductor

C. Orthogonality Principle

According to [21] skin and proximity losses can be summed if flux density B is assumed to be uniform on the conductor. Figure 5 shows the eddy currents induced by both skin effect and proximity effects.

Total losses are expressed as follows [22]:

$$P = \frac{l}{\sigma}\int_{t=0}^{T}\iint j^2 . dS . dt = \frac{l}{\sigma}\int_{t=0}^{T}\iint (j_s + j_p)^2 . dS . dt \quad (15)$$

$$P = \frac{l}{\sigma}\int_{t=0}^{T}\left[\iint {j_s}^2 + {j_p}^2 dS + \int_{-\frac{d}{2}}^{\frac{d}{2}}\int_{-\frac{d}{2}}^{\frac{d}{2}} 2 . j_s . j_p . dx . dy\right] dt \quad (16)$$

Considering uniform flux density on conductor, we can conclude from Figure 5 that:

$$j_p(y) = -j_p(-y) \quad (17)$$

$$j_s(y) = j_s(-y) \quad (18)$$

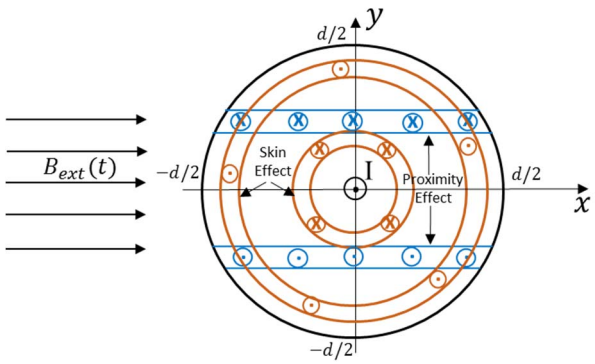

Figure 5 Eddy currents due to skin and proximity effect in round conductor

Then,

$$\int_{y=0}^{d/2}\int_{-d/2}^{d/2} 2 . j_s . j_p . dx . dy = -\int_{y=-d/2}^{0}\int_{-d/2}^{d/2} 2 . j_s . j_p . dx . dy \quad (19)$$

Finally,

$$P = \frac{l}{\sigma}\int_{t=0}^{T}\iint (j_s^2 + j_p^2) . dS . dt = P_{skin} + P_{proximity} \quad (20)$$

The orthogonality principle is applied to sum skin and proximity losses under the assumption of uniform flux density on the conductor. In order to respect this assumption, conductor's diameter is limited depending on the frequency as shown in Figure 4.

IV. Results

In this section, the studied machine is presented. FEM simulations are performed using 2D Transient solver of ANSYS Electronics Desktop 2018. Results obtained by hybrid model and FEM are provided in both no load and on load cases. The influence of slot opening is also investigated.

A. Studied Machine

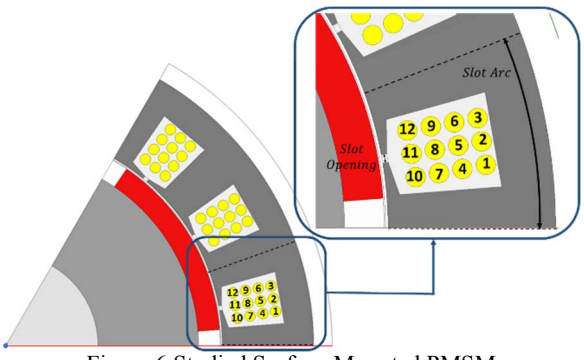

Figure 6 Studied Surface-Mounted PMSM

AC losses are evaluated for a one slot per pole per phase PMSM as shown in Figure 6. The stator lamination is configured with 18 slots and one-layer distributed winding. There are 12 copper turns with one strand in hand. The slot contains four horizontal layers with three copper turns in each. Table 1 presents additional details concerning studied SM-PMSM.

Table 1 Details of studied Surface-Mounted PMSM

Parameter	Value
Stator Outer Radius [mm]	100
Rotor Outer Radius [mm]	69.6
Active Length [mm]	250
Poles	6
Slots	18
Slots-per-pole-per-phase	1
Slot Opening [rad]	0.01
Air-gap Thickness [mm]	0.7

B. No Load Results

The flux density is bidirectional inside slots as shown in Figure 7. Figure 8 and Figure 9 show periodic waveform of both components of flux density inside conductors 4, 7, and 10. Results obtained show that waveform of flux density inside conductors is not sinusoidal and have a tangential component higher than radial component as shown in Figure 7. Hence, (8) cannot be applied in this case.

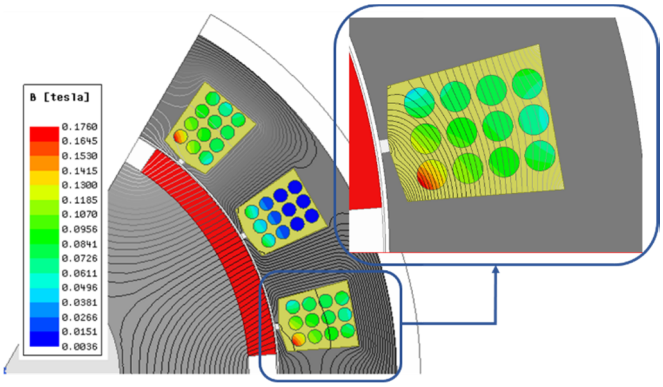

Figure 7 Flux lines and Flux density in Surface-Mounted PMSM (I=0A, $\Omega = 20\,000\,rpm$, $d = 3{,}5\,mm$)

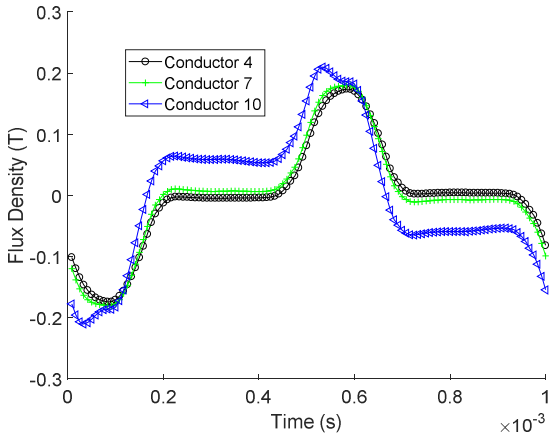

Figure 8 Periodic waveform of Tangential component of Flux Density inside conductors 4, 7, and 10 (I=0A, $\Omega = 20\,000\,rpm$)

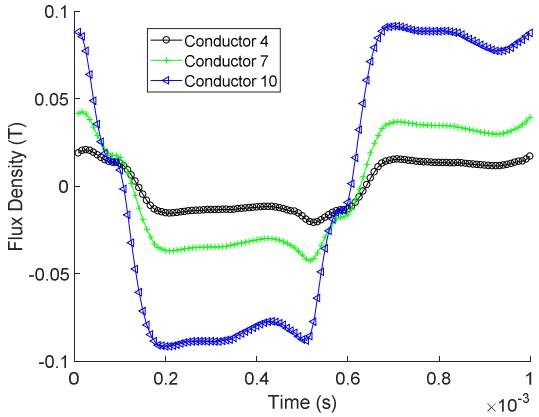

Figure 9 Periodic waveform of Radial component of Flux Density inside conductors 4, 7, and 10 (I=0A, $\Omega = 20\,000\,rpm$)

AC losses are calculated for different values of conductor's diameter and frequency. At no load, only proximity effect occurs in conductors. Figure 10 shows results obtained with both hybrid model and FEM.

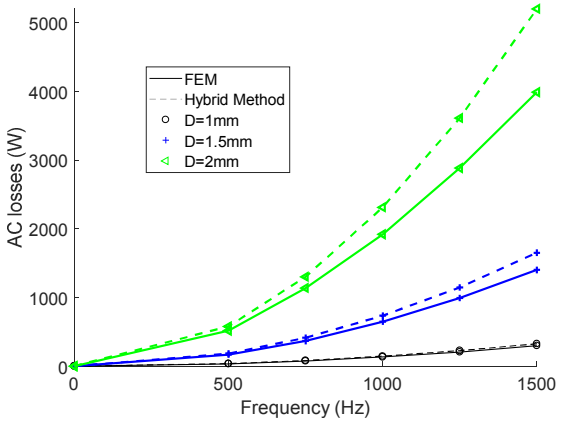

Figure 10 AC losses in conductors with FEM and Hybrid Method (I=0A)

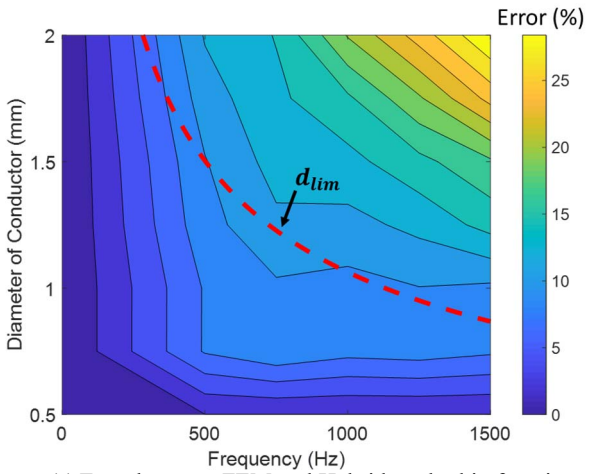

Figure 11 Error between FEM and Hybrid method in function of frequency and conductor's diameter (I=0A)

The error between FEM and hybrid method is shown in Figure 11. Maximum error is obtained at high diameter and high frequency. This is because the assumption of uniform flux density inside conductors, used for proximity losses formula, is less verified. In fact, this assumption is equivalent to (14) which corresponds to conductor's diameter limit in function of frequency represented by the red dashed line in Figure 11. The error between FEM and

hybrid model for frequencies and diameters values in this zone is less than 10%.

In order to evaluate the contribution of each harmonic in AC losses, (12) is used. Table 2 shows the results obtained. The contribution of third harmonic is at most of the time 56% of total proximity losses. Hence, AC losses cannot be evaluated in this case by considering sinusoidal waveform of flux density.

Table 2 Losses due to flux density harmonics (I=0A)

Speed (rpm)		10 000		20 000		30 000	
Diameter (mm)		0.5	1	0.5	1	0.5	1
AC losses (W)		2.26	36.12	9.04	144.48	20.34	325
Harmonic 1	Losses (W)	0.56	8.94	2.24	35.75	5.03	80.44
	% to AC losses	24%	24.7%	24.7%	24.7%	24.7%	24.7%
Harmonic 3	Losses (W)	1.27	20.37	5.1	81.47	11.48	183.31
	% to AC losses	56%	56.4%	56.4%	56.3%	56.4%	56.4%

C. *On Load Results*

In the on load case, both skin and proximity effects occur in the conductor because of flowing current and external alternating magnetic field. AC losses are calculated for different values of conductor's diameter and frequency. Figure 12 shows results obtained with both hybrid model and FEM. At f = 0, only joules losses occur in the conductor which explains highest losses for lowest conductor's diameter. However, at high frequency AC losses are higher for high conductor's diameter due to proximity effect as predicted by (11).

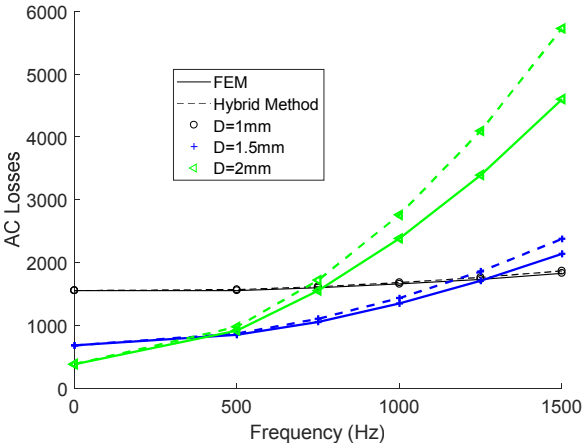

Figure 12 AC losses in conductors with FEM and Hybrid Method (I=50A)

Figure 13 shows the error between the two methods. Error is maximum at high diameter and high frequency. This is because the assumption of uniform flux density inside conductors, used for both proximity losses formula and orthogonality principle, is less verified. In fact, this assumption is equivalent to (14) which corresponds to conductor's diameter limit in function of frequency represented by the red dashed line in Figure 13. The error between FEM and hybrid model for frequencies and diameters values in this zone is less than 5%. Indeed, skin effect losses that occur only in on load case are accurately evaluated unlike proximity losses which requires uniformity of flux density inside conductors. For a large value range of frequency and conductor's diameter, skin losses have high contribution to AC losses, which explains a better accuracy of the hybrid method in the on load case.

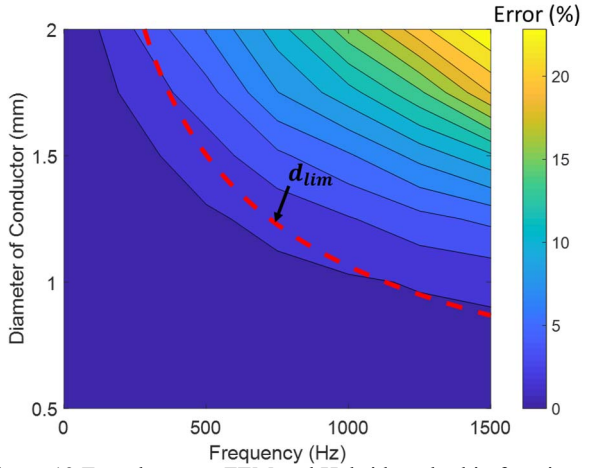

Figure 13 Error between FEM and Hybrid method in function of frequency and conductor's diameter (I=50A)

Table 3 shows DC losses, AC Losses, and the contribution of skin effect losses and proximity effect losses to AC losses. Additional losses due to skin effect are not remarkable for low values of γ as explained in Figure 2. Hence, skin effect losses are equal to DC losses.

Table 3 Losses due to flux density harmonics (I=50A)

Speed (rpm)		15 000			30 000		
Diameter (mm)		0.5	1	1.5	0.5	1	1.5
DC Losses (W)		6134	1533	681	6134	1533	681
AC losses		6139	1616	1104	6155	1866	2377
Skin Effect	Losses (W)	6134	1533	681	6134	1533	682
	% to AC losses	99.9%	95%	62%	99.6%	82%	29%
Proximity Effect	Losses (W)	5	83	423	21	333	1695
	% to AC losses	0.1%	5%	38%	0.4%	18%	71%

For higher conductor's diameter, skin effect losses decrease because R_{DC} decreases (1) while proximity losses increase as predicted by (12). Consequently, contribution of skin effect to AC Losses decreases for high conductor's diameter and contribution of proximity effect increases.

In addition, proximity effect losses increase remarkably with frequency as predicted by (12) unlike skin effect which is noticeable only at very high frequency as shown in Figure 2. Consequently, at high frequency and high conductor's diameter, proximity losses are dominant.

D. *Influence of Slot Opening*

The form of the slot affects strongly the path of flux lines inside the slot because of iron's high permeability. Hence, proximity effect losses depend on geometrical variables of the slot. In this section, we are going to study the influence of slot opening on proximity losses and on the accuracy of hybrid model for both on load and no load cases. The rotation speed of electrical machine is 20,000 rpm and conductor's diameter is 1 mm.

Figure 14 shows AC losses for different values of slot opening for no load and on load cases. In the no load case, it is concluded that the larger is the slot opening, the higher are proximity losses. This is mainly due to presence of magnets at the surface of the rotor that creates an alternating magnetic field that penetrates the conductors through the slot opening. In the on load case, it is noticed that the larger is the slot opening, the higher are AC losses. Knowing that skin effect losses are constant because they depend only on conductor's diameter, frequency and current value, it is concluded that increasing AC losses means increasing proximity effect losses. As mentioned above, this is mainly due to presence of magnets at the surface of the rotor.

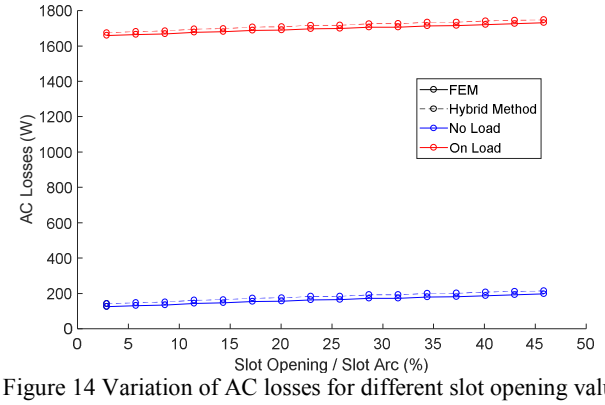

Figure 14 Variation of AC losses for different slot opening values with FEM and Hybrid Method

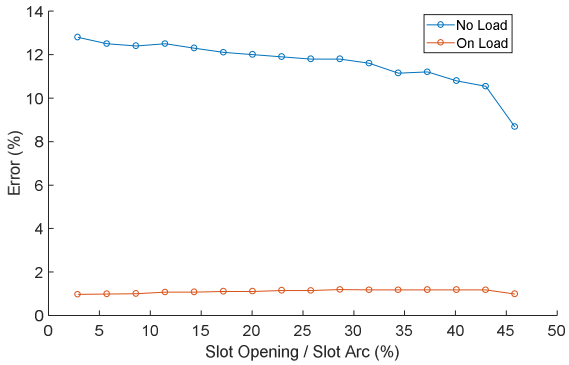

Figure 15 Error between FEM and Hybrid Method for different slot opening values (I=0A)

Figure 15 shows the error between hybrid model and FEM results of AC losses for different slot opening values for no load and on load cases. The hybrid model is still accurate for different values of slot opening. The error obtained is less than 13% for no load case and less than 1.2% for on load case. It is noticed that for on load case, the model is more accurate because the skin effect, which are dominant on large value range of conductor's diameter and frequency, are accurately evaluated.

V. CONCLUSION

Researchers are faced to many challenges when designing high speed electrical machines. One of the main problems is the limited voltage that leads to the use of a low number of conductors, thus with high diameter to keep same fill factor. However, due to noticeable skin effect in conductor with high diameters, one solution is to use multiple strands in hand. Hence, proximity effect becomes more important and should be well evaluated. Furthermore, the presence of magnets on the surface of the rotor causes the existence of alternating magnetic field flowing into conductors through slot openings. In order to accurately evaluate AC losses with less computation time, a hybrid model is proposed. The main outcomes of this model are the consideration of the two-dimensional and arbitrary waveforms of flux density inside slots.

The hybrid model is proved to give accurate results compared to FEM ones for a wide value range of conductor's diameter, frequency, and slot opening. This model will be included in a methodology of optimization and design of high-speed electrical machines. This methodology and the designed machines will be presented in future works.

VI. REFERENCES

[1] R. Missoum, N. Bernard, M. E. Zaim and J. Bonnefous, "Optimization of high speed surface mounted permanent magnet synchronous machines," in *International Aegean Conference on Electrical Machines and Power Electronics and Electromotion ACEMP'07 and Electromotion'07 Joint Conference*, 2007.

[2] M. E. El-Hadi Zaïm, H. Ben Ahmed and N. Bernard, "High-Speed Electric Machines," in *Non-conventional Electrical Machines*, John Wiley and Sons, 2013, pp. 117-189.

[3] X. Jannot, J. C. Vannier, C. Marchand, M. Gabsi, J. Saint-Michel and D. Sadarnac, "Multiphysic modeling of a high-speed interior permanent-magnet synchronous machine for a multiobjective optimal design," *IEEE Transactions on Energy Conversion,* vol. 26, no. 2, pp. 457-467, 2011.

[4] N. Boucenna, S. Hlioui, B. Revol and F. Costa, "Modeling of the propagation of high-frequency currents in AC motors," in *IEEE International Symposium on Electromagnetic Compatibility*, 2012.

[5] P. Ponomarev, I. Petrov, J. Pyrh and N. Bianchi, "Additional Losses in Stator Slot Windings of Permanent Magnet Synchronous Machines," no. May, pp. 1-11, 2015.

[6] P. Dowell, "Effects of eddy currents in transformer windings," *Proceedings of the Institution of Electrical Engineers,* vol. 113, no. 8, p. 1387, 1966.

[7] C. R. Sullivan, "Computationally efficient winding loss calculation with multiple windings, arbitrary waveforms, and two-dimensional or three-dimensional field geometry," *IEEE Transactions on Power Electronics,* vol. 16, no. 1, pp. 142-150, 1 2001.

[8] P. H. Mellor, R. Wrobel and N. McNeill, "Investigation of proximity losses in a high speed brushless permanent magnet motor," in *Conference Record - IAS Annual Meeting (IEEE Industry Applications Society)*, 2006.

[9] P. B. Reddy, T. M. Jahns and A. M. El-Refaie, "Impact of winding layer number and slot/pole combination on AC armature losses of synchronous surface PM machines designed for wide constant-power speed range operation," in *Conference Record - IAS Annual Meeting (IEEE Industry Applications Society)*, 2008.

[10] A. A. Arkadan, R. Vyas, J. G. Vaidya and M. J. Shah, "Effect of toothless stator design on core and stator conductors eddy current losses in permanent magnet generators," *IEEE Transactions on Energy Conversion,* vol. 7, no. 1, pp. 231-237, 1992.

[11] A. S. Thomas, Z. Q. Zhu and G. W. Jewell, "Proximity Loss Study In High Speed Flux-Switching Permanent Magnet Machine," *IEEE Transactions on Magnetics,* vol. 45, no. 10, pp. 4748-4751, 2009.

[12] P. B. Reddy, T. M. Jahns and T. P. Bohn, "Modeling and analysis of proximity losses in high-speed surface permanent magnet machines with concentrated windings," in *2010 IEEE Energy Conversion Congress and Exposition, ECCE 2010 - Proceedings*, 2010.

[13] A. Bellara, H. Bali, R. Belfkira, Y. Amara and G. Barakat, "Analytical prediction of open-circuit eddy-current loss in series double excitation synchronous machines," *IEEE Transactions on Magnetics,* vol. 47, no. 9, pp. 2261-2268, 9 2011.

[14] Y. Amara, P. Reghem and G. Barakat, "Analytical prediction of eddy-current loss in armature windings of permanent magnet brushless AC machines," in *IEEE Transactions on Magnetics*, 2010.

[15] L. J. Wu and Z. Q. Zhu, "Analytical investigation of open-circuit eddy current loss in windings of PM machines," in *Proceedings - 2012 20th International Conference on Electrical Machines, ICEM 2012*, 2012.

[16] P. B. Reddy, Z. Q. Zhu, S. H. Han and T. M. Jahns, "Strand-level proximity losses in PM machines designed for high-speed operation," in *Proceedings of the 2008 International Conference on Electrical Machines, ICEM'08*, 2008.

[17] S. Xu and H. Ren, "Analytical computation for AC resistance and reactance of electric machine windings in ferromagnetic slots," *IEEE Transactions on Energy Conversion,* vol. 33, no. 4, pp. 1855-1864, 1 12 2018.

[18] G. Volpe, M. Popescu, F. Marignetti and J. Goss, "Modelling AC Winding Losses in a PMSM with High Frequency and Torque Density," in *2018 IEEE Energy Conversion Congress and Exposition, ECCE 2018*, 2018.

[19] S. Ramo, J. R. Whinnery and V. Twersky, Fields and Waves in Modern Radio, vol. 7, AIP Publishing, 1954.

[20] P. S. Venkatraman, "Winding eddy current losses in switch mode power transformers due to rectangular wave currents," *in Proc. Powercon 11,* Vols. Section A-1, pp. 1-11, 1984.

[21] G. Bertotti, D. Chiarabaglio, F. Fiorillo, A. Boglietti, M. Chiampi and M. Lazzari, "An improved estimation of iron losses in rotating electrical machines," *IEEE Transactions on Magnetics,* vol. 27, no. 6, pp. 5007-5009, 1991.

[22] J. A. Ferreira, "Appropriate modelling of conductive losses in the design of magnetic components," in *PESC Record - IEEE Annual Power Electronics Specialists Conference*, 1990.

VII. BIOGRAPHIES

Taha El Hajji is currently working toward the Ph.D. degree at SATIE laboratory of the Ecole Normale Superieure Paris Saclay, France and Groupe PSA. His work is focused on high-speed electrical machines for electric vehicles. He received the master of engineering degree in electrical engineering and automation from ENSEEIHT, Toulouse, France, in 2018. He received the master of research in automotive electrification and propulsion from Ecole Normale Supérieure Paris-Saclay, Gif-sur-Yvette, France, in 2018.

Sami Hlioui received the M.Sc. degree in electrical engineering from the Ecole Normale Superieure de Cachan, France, in 2005, the Ph.D. degree in electrical power engineering from the University of Technology of Belfort-Montbeliard, Belfort, France, in 2008 and the HDR degree from Ecole Normale Superieure de Cachan, France, in 2018.
He is a Lecturer with the Conservatoire National des Arts et Métiers (Le Cnam), Paris, France, and a Researcher with the Laboratory of Systems and Applications of Information and Energy Technologies, SATIE, France. His main research interests include the multidisciplinary modeling of electromagnetic actuators and the optimal design of these actuators for embedded applications

François Louf received the Ph.D. degree in mechanical engineering from the Ecole Normale Supérieure de Cachan, (Cachan, France), in 2003, He received the HDR from the Ecole Normale Supérieure de Paris-Saclay, (Cachan, France), in 2017. He was an Assistant Professor at Paris X Nanterre,Nanterre, France, in 2003. Since 2005, he has been with the LMT laboratory, ENS Paris-Saclay. His main research interests are model validation, uncertainties in finite-element models, and model updating with real-time constraints.

Mohamed Gabsi received the Ph.D. degree in electrical engineering from the University of Paris-VI, Paris, France, in 1987, and the HDR degree from the University of Paris-XI, Orsay, France, in 1999. Since 1990, he has been working with the electrical machines team SETE of the Laboratory of Systems and Applications of Information and Energy Technologies, Ecole Normale Superieure de Cachan, Cachan, France, where he is currently a Full Professor. His research interests include switched reluctance motor, vibrations and acoustic noise, and permanent magnet machines.

Guillaume Mermaz-Rollet received an Engineer degree in powertrain engineering from IFP School (France) in 2002. He also received an Engineer degree in mechanical engineering from Ecole Nationale Supérieure d'Arts et Métiers (France) in 2001. He works at Groupe PSA since 2002 as powertrain engineer. He is currently in research department.

M'Hamed Belhadi received a PhD degree in Paris Sud university in 2015 (France) on electrical machine and a master 2 research in electrical engineering from Polytech'Nantes (University of Nantes, France) in 2011. He also received an Engineer degree in electromechanical engineering from Bejaia University, Algeria, in 2010. He is currently an innovation engineer at Groupe PSA, France.